

Geometrically Nonlinear Random Responses of Stiffened Plates Under Acoustic Pressure

YANG Shaochong¹, LI Youchen¹, YANG Qingsheng^{2*}, WANG Jianmin³

1. College of Civil Engineering and Architecture, Hebei University, Baoding 071002, P.R. China;

2. Department of Engineering Mechanics, Beijing University of Technology, Beijing 100124, P.R. China;

3. Science and Technology on Reliability and Environment Engineering Laboratory, Beijing Institute of Structure and Environment Engineering, Beijing 100076, P.R. China

(Received 10 June 2020; revised 20 July 2020; accepted 1 September 2020)

Abstract: An algorithm integrating reduced order model (ROM), equivalent linearization (EL), and finite element method (FEM) is proposed to carry out geometrically nonlinear random vibration analysis of stiffened plates under acoustic pressure loading. Based on large deflection finite element formulation, the nonlinear equations of motion of stiffened plates are obtained. To reduce the computation, a reduced order model of the structures is established. Then the EL technique is incorporated into FE software NASTRAN by the direct matrix abstraction program (DMAP). For the stiffened plates, a finite element model of beam and plate assembly is established, in which the nodes of beam elements are shared with shell elements, and the offset and section properties of the beam are set. The presented method can capture the root-mean-square (RMS) of the stress responses of shell and beam elements of stiffened plates, and analyze the stress distribution of the stiffened surface and the unstiffened surface, respectively. Finally, the statistical dynamic response results obtained by linear and EL methods are compared. It is shown that the proposed method can be used to analyze the geometrically nonlinear random responses of stiffened plates. The geometric nonlinearity plays an important role in the vibration response of stiffened plates, particularly at high acoustic pressure loading.

Key words: stiffened plate; acoustic loading; geometric nonlinearity; random vibration; equivalent linearization

CLC number: O322;O324

Document code: A

Article ID: 1005-1120(2020)05-0726-13

0 Introduction

Stiffened plates and shells are common structural forms used in the aerospace industry^[1], owing to their many advantages over unstiffened plates, such as their very high stiffness to weight ratio. Stiffened panel usually consists of a basic structure and local reinforcement elements called stiffeners are added to improve the static and dynamic characteristics of the structure. The behavior of stiffened plate structures subjected to linear random vibrations under low levels of acoustic excitation is readily determined because approximate solutions of the equations of motion are readily obtained under these conditions.

However, stiffened plates readily sustain large amplitude vibrations when subjected to excessive acoustic excitation. In this case, the structural stiffness employed in the equations of motion governing a plate is dependent upon the magnitude of deflection, making the equations of motion nonlinear, and difficult to solve. In addition, the structural discontinuity and anisotropy are induced by stiffeners. This unique characteristic makes the nonlinear random vibration response analyses much more complicated than those of the unstiffened plate. For these reasons, the equations of motion are far more complex in the case of nonlinear random vibrations, and obtaining approximate solutions in a computationally

*Corresponding author, E-mail address: qsyang@bjut.edu.cn.

How to cite this article: YANG Shaochong, LI Youchen, YANG Qingsheng, et al. Geometrically nonlinear random responses of stiffened plates under acoustic pressure[J]. Transactions of Nanjing University of Aeronautics and Astronautics, 2020, 37(5):726-738.

<http://dx.doi.org/10.16356/j.1005-1120.2020.05.007>

efficient manner is very difficult. Therefore, the development of theoretical models and computationally efficient approaches for obtaining reasonably accurate approximate solutions of nonlinear motion equations is essential for achieving a thorough understanding of the nonlinear random vibration response of stiffened plates under acoustic loads.

Numerous studies of the vibration characteristics of stiffened plates have been conducted using various theoretical models and solution approaches. Ma et al.^[2] investigated the nonlinear forced vibration of the stiffened plates with four clamped edges based on the Lagrange equation and the energy principle. Chen et al.^[3] investigated the strongly nonlinear free vibration of four edges simply supported stiffened plates with geometric imperfections. Cho et al.^[4] dealt with numerical procedure for the vibration analysis of rectangular plates and stiffened panels subjected to point excitation force and enforced displacement at boundaries. Sheikh and Mukhopadhyay^[5-6] investigated the geometric nonlinearity of stiffened plates by the spline finite strip method, and applied this method to analyze linear and nonlinear transient vibration of plates and stiffened plates. Mitra et al.^[7] studied the influence of stiffener position, plate aspect ratio, and stiffener to plate thickness ratio on the large amplitude dynamic behavior. Qing et al.^[8] developed a novel mathematical model for free vibration analysis of stiffened laminated plates by separate consideration of plate and stiffeners based on the semi-analytical solution of the state-vector equation theory. Li et al.^[9] proposed the Karhunen-Loeve expansion (KLE), finite element method (FEM), and boundary element method (BEM) (KLE/FEM/BEM) to carry out vibro-acoustic analysis of stiffened panel under stationary and non-stationary random excitations. Dogan^[10] used the Galerkin type approach to study the nonlinear vibration of clamped functionally graded material plates under random excitation, but it is difficult to apply this method to the systems with complex geometry and boundary conditions.

One of the most widely used approximation techniques for the random problem is the equivalent

linearization (EL) that the nonlinearities in system are replaced by effective linear systems. The advantage of the EL method is that it can be combined with FEM and applied to nonlinear systems with complex geometry and boundary conditions. Robinson et al.^[11] predicted the nonlinear random response of structures using an EL technique by means of the direct matrix abstraction program (DMAP) modifications in NASTRAN. While it is possible to perform an EL analysis in the physical degrees-of-freedom, it is desirable to transform the problem into modal coordinates to simplify the problem.

One approach for reducing the computational burden associated with solving ordinary differential equations is to reduce the order of the equations using the mode summation method. Here, a physical multiple degree of freedom system is translated into a modal system, which is convenient for analyzing its nonlinear random vibrations. The appropriate selection of modal basis vectors and the determination of nonlinear stiffness coefficients in the reduced-order equations are essential aspects of this approach. Rizzi and Przekop^[12] investigated the effect of modal basis selection on geometric nonlinear response prediction using a reduced-order nonlinear modal simulation. Przekop et al.^[13] examined three procedures for guiding the selection of an efficient modal basis in a nonlinear random response analysis. Kim et al.^[14] developed nonlinear structural dynamic reduced-order models of beams and plates, and established their validity. Mignolet et al.^[15] presented an extensive review of indirect methods for the construction of reduced-order models employed for the prediction of the vibration responses of geometrically nonlinear structures represented by finite element models. Parandvar and Farid^[16] studied the large amplitude vibration of functionally graded material plates subjected to combined random pressure and thermal loadings using the finite element modal reduction method. Przekop and Rizzi^[17] adopted a reduced-order method to investigate the geometrically nonlinear response of structures exposed to combined loadings, and investigated the effect of modal basis se-

lection on the quality of the results obtained.

The numerical results for a thin simply-supported aluminum plate^[18] are in good agreement with previously reported data in Refs. [19-20], which confirms that the proposed method has reasonable precision and high efficiency. But the implement method is not applied to stiffened plate. It should be pointed out that Solution 106 cannot analyze the large deformation of the stiffened plate with offset and the nonlinear nodal forces cannot be obtained. So, the nonlinear nodal forces of the stiffened plate need to be solved in Solution 400. In this paper the implementation method proposed in Ref.[18] is improved, and then it is applied to stiffened plates.

This paper is organized as follows. In Section 1, the large deflection finite element formulations of stiffened plates are briefly introduced to establish the general nonlinear equations of motion. In Section 2, the EL method for geometrically nonlinear random vibration is introduced, and an improved implementation of the EL method is presented. In Section 3, a numerical example, including linear and geometrically nonlinear random vibration analyses of stiffened plates, is given. Finally, the main conclusions are summarized in Section 4.

1 Reduced Order Model of Geometrically Nonlinear Structures

The system mass, damping and stiffness matrices are generally obtained using a commercial finite element software. But the nonlinear stiffness which is related to \mathbf{F}_T , is not available within a commercial finite element software. The equations of motion of a multiple degree-of-freedom, viscously damped geometrically nonlinear system can be written in the form

$$\begin{aligned} & \mathbf{M}\ddot{\mathbf{X}}(t) + \mathbf{C}\dot{\mathbf{X}}(t) + \mathbf{K}\mathbf{X}(t) + \\ & (\mathbf{K}_1\mathbf{X}(t) + \mathbf{K}_2\mathbf{X}\mathbf{X}^T(t))\mathbf{X}(t) = \mathbf{P}(t) \end{aligned} \quad (1)$$

or in more general form, as

$$\mathbf{M}\ddot{\mathbf{X}}(t) + \mathbf{C}\dot{\mathbf{X}}(t) + \mathbf{K}\mathbf{X}(t) + \mathbf{F}(\mathbf{X}(t)) = \mathbf{P}(t) \quad (2)$$

where the matrices \mathbf{M} , \mathbf{C} and \mathbf{K} are the mass, proportional damping, and linear stiffness matrices, respectively. $\mathbf{X}(t)$ is the displacement response vector

and $\mathbf{P}(t)$ the force excitation vector. The coefficients \mathbf{K}_1 and \mathbf{K}_2 are the system first and second-order nonlinear stiffness coefficients. For the problems of interest, the nonlinear restoring force vector \mathbf{F} can be adequately represented by quadratic and cubic order terms in \mathbf{X} .

Performing an EL analysis in the physical degrees-of-freedom is very difficult. To reduce the computational cost and time, a modal equation with reduced degrees-of-freedom is obtained by applying the modal coordinate transformation

$$\mathbf{X}(t) = \mathbf{\Phi}\mathbf{q}(t) \quad (3)$$

to Eq.(2), a modal equation of motion can be written as

$$\begin{aligned} & \widetilde{\mathbf{M}}\ddot{\mathbf{q}}(t) + \widetilde{\mathbf{C}}\dot{\mathbf{q}}(t) + \widetilde{\mathbf{K}}\mathbf{q}(t) + \widetilde{\mathbf{F}}(q_1, q_2, \dots, q_L) = \\ & \widetilde{\mathbf{P}}(t) \end{aligned} \quad (4)$$

where

$$\begin{aligned} & \widetilde{\mathbf{M}} = \mathbf{\Phi}^T \mathbf{M} \mathbf{\Phi} = [\mathbf{I}] \quad \widetilde{\mathbf{C}} = \mathbf{\Phi}^T \mathbf{C} \mathbf{\Phi} = [2\zeta_r \omega_r] \\ & \widetilde{\mathbf{K}} = \mathbf{\Phi}^T \mathbf{K} \mathbf{\Phi} = [\omega_r^2] \quad \widetilde{\mathbf{F}} = \mathbf{\Phi}^T \mathbf{F} \quad \widetilde{\mathbf{P}} = \mathbf{\Phi}^T \mathbf{P} \end{aligned} \quad (5)$$

where q_1, q_2, \dots, q_L are the components of \mathbf{q} , and \mathbf{q} is the vector of modal coordinates. ζ_r is the viscous damping factors, ω_r the undamped natural frequencies, and $\mathbf{\Phi}$ generally the subset of the linear eigenvectors obtained from Eq.(2) without \mathbf{F} . A normal modes analysis was performed to obtain the modal matrixes, from which modes with relatively high modal effective mass fraction were selected as the modal base vectors to reduce order of the equations of motion^[21].

The nonlinear restoring force components in modal space are replaced by the product of quadratic and cubic nonlinear modal displacements multiplied by unknown nonlinear modal stiffness coefficients. In the present paper, the assumed form of the nonlinearities will be cubic based upon previous studies of aircraft structural response^[22]. Thus, it can be written as

$$\begin{aligned} & \widetilde{\mathbf{F}}_r(q_1, q_2, \dots, q_L) = \sum_{j=1}^L \sum_{k=j}^L \sum_{l=k}^L b_{jkl}^r q_j q_k q_l \\ & r = 1, 2, \dots, L \end{aligned} \quad (6)$$

where L is the number of modal base vectors. This form is sufficient for characterizing the type of nonlinearity of interest in this paper and facilitates the subsequent solution of the equivalent linear system.

The particular displacement fields are given for a series of inverse linear and nonlinear static analysis to determine the coefficients $b_{jkl}^{[19,23]}$. The total nodal force F_T may be written in physical coordinates as

$$F_T = F_L + F_{NL} = \mathbf{K}X_c + \mathbf{F}(X_c) \quad (7)$$

where X_c is a prescribed physical nodal displacement vector, and F_L and F_{NL} are the linear and nonlinear contributions to the total nodal force. F_L is first obtained by prescribing X_c in the linear static solution. F_T is then obtained by prescribing X_c in the nonlinear static solution which includes both the linear and nonlinear contributions. Note in linear analysis, assuming the displacements are small and the nonlinear terms are negligible, the nodal force vector is $F_L = \mathbf{K}X_c$. Finally, the nonlinear contribution F_{NL} is obtained by subtracting F_L from F_T , or

$$F_{NL} = \mathbf{F}(X_c) = F_T - F_L \quad (8)$$

One can begin by prescribing the displacement fields

$$X_c = +\phi_1 q_1 \quad (9)$$

where ϕ_i is mode shape vector (eigenvector). The nonlinear nodal force contributions F_{NL} are determined using Eq.(8) after solving the linear and nonlinear static solutions. These may be written in modal coordinates as

$$\tilde{F}_{NL} = \mathbf{\Phi}^T F_{NL} = \mathbf{\Phi}^T \mathbf{F}(+\phi_1 q_1) = [b_{111}^r] q_1 q_1 q_1 \quad (10)$$

where the sought stiffness coefficients $[b_{111}^r]$ are vectors of length L . Note that the other nonlinear terms do not appear in Eq.(10) since $q_j = 0$ for $j \neq 1$. Since q_1 is a known scalar, the coefficients $[b_{111}^r]$ for $r = 1, 2, \dots, L$ can be determined from the resulting system Eq.(10) of L linear equations. The remaining coefficients $[b_{jjj}^r]$ for ($j = 2, 3, \dots, L$) can be determined in an analogous manner.

A similar technique can be used to determine stiffness coefficients with two unequal lower indices, e.g. $[b_{112}^r]$ and $[b_{122}^r]$. Coefficients of this type appear only if the number of retained eigenvectors is greater than or equal to two ($L \geq 2$). Prescribing the displacement fields

$$\begin{aligned} X_{c1} &= +\phi_1 q_1 + \phi_2 q_2 \\ X_{c2} &= +\phi_1 q_1 - \phi_2 q_2 \end{aligned} \quad (11)$$

results in the following equations

$$\begin{aligned} \tilde{F}_{NL_1} &= \mathbf{\Phi}^T F_{NL_1} = \mathbf{\Phi}^T \mathbf{F}(+\phi_1 q_1 + \phi_2 q_2) = \\ & [b_{111}^r] q_1 q_1 q_1 + [b_{222}^r] q_2 q_2 q_2 + \\ & [b_{112}^r] q_1 q_1 q_2 + [b_{122}^r] q_1 q_2 q_2 \\ \tilde{F}_{NL_2} &= \mathbf{\Phi}^T F_{NL_2} = \mathbf{\Phi}^T \mathbf{F}(+\phi_1 q_1 - \phi_2 q_2) = \\ & [b_{111}^r] q_1 q_1 q_1 - [b_{222}^r] q_2 q_2 q_2 - \\ & [b_{112}^r] q_1 q_1 q_2 + [b_{122}^r] q_1 q_2 q_2 \end{aligned} \quad (12)$$

The first equation of Eq.(12) plus or minus the second, results in

$$\begin{aligned} \tilde{F}_{NL_1} + \tilde{F}_{NL_2} &= +2[b_{111}^r] q_1 q_1 q_1 + 2[b_{122}^r] q_1 q_2 q_2 \\ \tilde{F}_{NL_1} - \tilde{F}_{NL_2} &= +2[b_{222}^r] q_2 q_2 q_2 + 2[b_{112}^r] q_1 q_1 q_2 \end{aligned} \quad (13)$$

From Eq.(13), the coefficients $[b_{112}^r]$ and $[b_{122}^r]$ may be determined from the $2 \times L$ system of equations. In this manner, all coefficients of the type $[b_{jkk}^r]$ and $[b_{kjj}^r]$ for $j, k = 1, 2, \dots, L$ may be found. For cases when the number of retained eigenvectors is greater than or equal to three ($L \geq 3$), coefficients with three unequal lower indices, e.g. $[b_{123}^r]$, may be determined by prescribing the displacement field

$$X_c = +\phi_1 q_1 + \phi_2 q_2 + \phi_3 q_3 \quad (14)$$

The resulting equation

$$\begin{aligned} \tilde{F}_{NL} &= \mathbf{\Phi}^T F_{NL} = \mathbf{\Phi}^T \mathbf{F}(+\phi_1 q_1 + \phi_2 q_2 + \phi_3 q_3) = \\ & [b_{111}^r] q_1 q_1 q_1 + [b_{222}^r] q_2 q_2 q_2 + [b_{333}^r] q_3 q_3 q_3 + \\ & [b_{112}^r] q_1 q_1 q_2 + [b_{221}^r] q_2 q_2 q_1 + [b_{113}^r] q_1 q_1 q_3 + \\ & [b_{331}^r] q_3 q_3 q_1 + [b_{223}^r] q_2 q_2 q_3 + [b_{332}^r] q_3 q_3 q_2 + \\ & [b_{123}^r] q_1 q_2 q_3 \end{aligned} \quad (15)$$

contains one column of unknown coefficients $[b_{123}^r]$. All coefficients of type $[b_{jkl}^r]$ ($j \neq k \neq l$) can be found in this manner.

The nonlinear stiffness coefficients b_{jkl} in Eq.(6) were obtained using a Fortran computer code denoted as nonlinear stiffness evaluation (NLSE). As a result, the implicit geometrically nonlinear equation of motion is represented as an explicit equivalent nonlinear equation of motion in modal coordinates. For a random loading, the solution of Eq.(4) with the nonlinear terms can be undertaken through numerical simulation or EL method. In this study the EL method is considered below.

2 Force Error Minimization of Equivalent Linearization Method for Random Loading

2.1 Theoretical foundation

Eq.(2) has no general solution when the excitation is random. An approximate solution can be obtained by using formation of an equivalent linear system

$$M\ddot{X}(t) + C\dot{X}(t) + [K + K_e]X(t) = P(t) \quad (16)$$

where K_e is the equivalent linear stiffness matrix. While it is possible to perform an EL analysis in the physical degrees of freedom, it is desirable to recast the problem in modal coordinates to simplify the problem. The equivalent linear analog of Eq.(4) may be found by applying Eq.(3) to Eq.(16)

$$\tilde{M}\ddot{q} + \tilde{C}\dot{q} + [\tilde{K} + \tilde{K}_e]q = \tilde{P} \quad (17)$$

where the modal equivalent linear stiffness matrix \tilde{K}_e is given by

$$\tilde{K}_e = \Phi^T K_e \Phi \quad (18)$$

The traditional force-error minimization method of EL was adopted to seek the minimizing between the nonlinear force and the product of the modal equivalent linear stiffness and displacement response vector. The error in the approximate system is defined as

$$\Delta = \tilde{F} - \tilde{K}_e q \quad (19)$$

Since the error is a random function of time, the required condition is that the expectation of the mean square error be a minimum. This is expressed as

$$E[\Delta^T \Delta] \rightarrow \min \quad (20)$$

where $E[\cdot]$ represents the expectation operator. Eq.(20) will be satisfied if

$$\frac{\partial E[\Delta^T \Delta]}{\partial \tilde{K}_{eij}} = 0 \quad i, j = 1, 2, \dots, N \quad (21)$$

where \tilde{K}_{eij} is the elements of matrix \tilde{K}_e and N the number of physical degrees of freedom. Substituting Eq.(19) into Eq.(21), and interchanging the expectation and differentiation operators, we have

$$E[\tilde{F} q^T] = E[q^T q] \tilde{K}_e^T \quad (22)$$

Using the fact that the matrix $E[\tilde{F} q^T]$ is non-singular, the matrix \tilde{K}_e can be determined

$$\tilde{K}_e = E[q^T q]^{-1} E[\tilde{F} q^T] \quad (23)$$

The matrix \tilde{K}_e defined in Eq.(23) can be directly obtained in a finite element code if the stiffness coefficients a and b are available and the expectation operator can be evaluated. It is generally assumed that a Gaussian excitation also has a Gaussian response. By using the formula for the expected value of a Gaussian vector q , the following relation can be obtained.

$$E[\tilde{F} q^T] = E[q^T q] E[\nabla \tilde{F}] \quad (24)$$

where ∇ is the gradient operator. In this method, the equivalent linear stiffness in modal coordinates may be written as

$$\tilde{K}_e = \left[E \left[\frac{\partial \tilde{F}}{\partial q} \right] \right] \quad (25)$$

where \tilde{F} is defined by Eq.(6) using the nonlinear modal stiffness coefficients. \tilde{K}_e is an equivalent linear function of the displacement vector q , which is one order less than the nonlinear system stiffness matrix \tilde{F} .

2.2 Iterative solution for modal equivalent linear stiffness matrix

Because the matrix \tilde{K}_e is a function of the unknown modal displacement response (covariance matrix), the solution to Eq.(17) takes an iterative form, i.e.

$$\tilde{M}\ddot{q}^m + \tilde{C}\dot{q}^m + [\tilde{K} + \tilde{K}_e^{m-1}]q^m = \tilde{P} \quad (26)$$

where superscript m is the iteration number. At the start of the first iteration \tilde{K}_e is equal to zero. Assuming stationary excitation, a stationary response is sought precluding the need for initial conditions. Note that in modal coordinates, the order of these matrices is not large, so it is not difficult to calculate the frequency response matrix $H(\omega)$ at each frequency, i.e.

$$H^{m-1} = (-\omega^2 \tilde{M} + i\omega \tilde{C} + \tilde{K} + [\alpha \tilde{K}_e^{m-1} + \beta \tilde{K}_e^{m-2}])^{-1} \quad (27)$$

The introduction of the weightings α and β is to aid in the convergence of the solution, with the condition that $\alpha + \beta = 1$. As discussed in Ref.[18], the weightings α and β played a significant role in the convergence of the iterative procedure. The appropriate values for α and β were adopted at various

acoustic pressure levels. In this paper, two variable values of α and β for optimizing the convergence rate at high acoustic pressure levels are developed to decrease the step size and avoid divergence.

For the random vibration of linear system Eq. (26), the spectral density matrices of the modal response S_{qq} and excitation \tilde{S}_{ff} are related by

$$S_{qq}^m = H^{m-1}(\omega) \tilde{S}_{ff} (\overline{H}^{m-1}(\omega))^T \quad (28)$$

where \tilde{S}_{ff} is the spectral density matrix of the load in modal coordinates, it can be written as

$$\tilde{S}_{ff} = \Phi^T S_{ff} \Phi \quad (29)$$

The spectral density matrix of the loading in physical degrees of freedom is the product of frequency response load vector f multiplied by its complex conjugate transpose \bar{f}^T

$$S_{ff} = f \bar{f}^T \quad (30)$$

where the over-bar in Eqs. (28, 30) indicates the complex conjugate, and f is the frequency response load vector. The zero-time-lag covariance matrix components $E[q_r q_s]$ are calculated from the response spectral density matrix using the Wiener-Khinchin formula. For the r, s components, this is written as

$$E[q_r q_s]^m = \sum_n S_{q_r q_s}^m \Delta \omega_n \quad (31)$$

Again, we note that the orders of matrices are not large in modal coordinates, so it is not difficult to calculate the covariance matrix by a simple numerical integration over frequency. After having done so, the updated \tilde{K}_e may be calculated as a function of the response covariance matrix

$$\tilde{K}_e^m = f(E[q_j q_k]^{m-1}) \quad (32)$$

For example, \tilde{K}_e for the m -th iteration of the force-error minimization approach is determined from Eq.(25) as

$$\tilde{K}_e^m = \left[E \left[\frac{\partial \tilde{\Gamma}}{\partial q} \right] \right]^m = \begin{bmatrix} E \left[\frac{\partial \{\tilde{\Gamma}_1\}}{\partial \{q_1\}} \right]} & \cdots & E \left[\frac{\partial \{\tilde{\Gamma}_1\}}{\partial \{q_L\}} \right]} \\ \vdots & \ddots & \vdots \\ E \left[\frac{\partial \{\tilde{\Gamma}_L\}}{\partial \{q_1\}} \right]} & \cdots & E \left[\frac{\partial \{\tilde{\Gamma}_L\}}{\partial \{q_L\}} \right]} \end{bmatrix} \quad (33)$$

Substitution of Eq.(6) into Eq.(33) yields

$$\tilde{K}_e^m = \begin{bmatrix} \sum_{j=1}^L \sum_{k=j}^L b_{jk1}^1 E[q_j q_k] & \cdots & \sum_{j=1}^L \sum_{k=j}^L b_{jkL}^1 E[q_j q_k] \\ \vdots & \ddots & \vdots \\ \sum_{j=1}^L \sum_{k=j}^L b_{jk1}^L E[q_j q_k] & \cdots & \sum_{j=1}^L \sum_{k=j}^L b_{jkL}^L E[q_j q_k] \end{bmatrix}^{m-1} \quad (34)$$

The iterations continue until the following convergence criterion is met

$$\frac{\sum_{j=1}^L \sum_{k=1}^L |\tilde{K}_{ejk}^m - \tilde{K}_{ejk}^{m-1}|}{L^2 |\tilde{K}_e^m|_{\max}} < e \quad (35)$$

where $|\tilde{K}_e^m|_{\max}$ is the entry of \tilde{K}_e^m with the largest absolute value, and the value of e is typically 0.001. Following convergence in \tilde{K}_e (and thus in $E[qq]$), the $N \times N$ covariance matrix of the displacements in physical coordinates is recovered by the transformation

$$E[x_i x_j] = \Phi E[q_r q_s] \Phi^T \quad (36)$$

and RMS values are the square roots of the diagonal terms in Eq.(36). Further post-processing to obtain power spectral densities of displacements, stresses, strains, etc., may be performed by substituting the converged equivalent stiffness matrix \tilde{K}_e into Eq.(17) and solving in the usual linear fashion.

2.3 Implementation of equivalent linearization solution

The whole implementation process is referred to Ref.[18]. It should be noted that the process of determining the nonlinear stiffness coefficient of stiffened plate is different from that of flat plate.

The present computer codes NLSE which mentioned in Ref.[18] was verified to be valid in plane structure. However, the implement method is not applicable to the stiffened plate. The Solution 106, which is called in the method, cannot analyze the large deformation problem of the stiffened plate, and the nonlinear node-force of its finite element model cannot be obtained. In order to solve this problem, the Solution 400 should be called and the options of "large deformation and large strain" and "stiffness varies with deformation" should be selected in the parameter setting to obtain the nonlinear

node-force of the finite element model of the stiffened plate^[24]. Here, the improved NLSE is applied to stiffened plates. The nonlinear stiffness coefficients are determined by performing a series of inverse linear static (Solution 101) and nonlinear static (Solution 400) solutions using particular displacement fields as previously described.

In this paper, we treat the acoustic excitation as random pressure acting on the surface of the plate. It is taken as uniformly distributed and varies in time. Acoustic pressure RMS and spectral density value corresponding to different sound pressure levels from 106 to 160 dB are shown in Table 1.

Table 1 Acoustic pressure RMS and spectral density value corresponding to different sound pressure levels

SPL/ dB	Acoustic pressure RMS/Pa	Single-sided value of spectral density/ (Pa ² •Hz ⁻¹)	Single-sided value of spectral density/ (Pa ² •rad ⁻¹ •s ⁻¹)
106	4	0.015 625	0.002 486 8
112	8	0.062 5	0.009 947 2
118	16	0.25	0.039 788 7
124	32	1	0.159 154 9
130	64	4	0.636 619 8
136	128	16	2.546 479 1
142	256	64	10.185 916
148	512	256	40.743 665
154	1 024	1 024	162.974 66
160	2 048	4 096	651.898 65

3 Numerical Example

3.1 Finite element model of stiffened plate and nonlinear stiffness coefficient

We consider a simply-supported rectangular aluminum stiffened plate. The plates and beams of the stiffened plates structure are discretized into two-dimensional plane elements and one-dimensional beam elements respectively for analysis. Beam and plate can share nodes and beam offset distance can be set. The stiffness matrices of the stiffened plates are composed by the addition of the respective plate and beam element stiffness matrices. The dimensions and material parameters of the plate are provided in Table 2. A NASTRAN model of the stiffened

Table 2 Dimensions and material properties of stiffened plate

Parameter	Value
Length of the plate / m	0.355 6
Width of the plate / m	0.254
Thickness of the plate / m	0.001
Cross section of beam $b \times h$ / (mm \times mm)	1 \times 2.968 2
Elastic modulus E / Pa	7.3×10^{10}
Poisson's ratio ν	0.3
Mass density of aluminum ρ / (kg \cdot m ⁻³)	2 763

plate is built with a uniform 20 \times 28 mesh composed of 560 CQUAD4 elements 48 beam elements and 609 nodes. The finite element model of the stiffened plate is shown in Fig.1(a), and the cross-sectional area of the beam is shown in Fig.1(b). The beam, plane element and joint at central position of the stiffened plate are shown in Fig.2. The mode shape, frequency (f) and modal effective mass fraction (η) of metal stiffened plates are shown in Table 3. It can be seen that the modal effective mass fraction of symmetrical modes (1, 5, 7, 11) is larger.

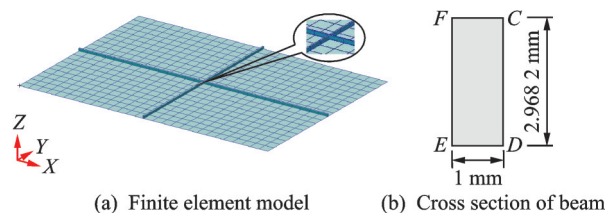


Fig.1 Stiffened plate model

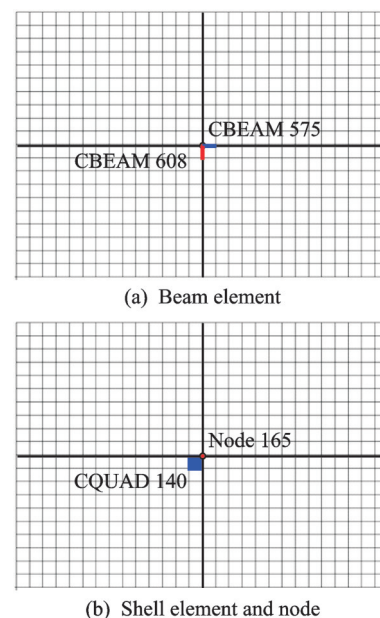


Fig.2 Beam and shell elements at the center position

Table 3 Mode shape, frequency and modal effective mass fraction of metal stiffened plate

Mode number	f/Hz	$\eta/\%$	Mode shape	Mode number	f/Hz	$\eta/\%$	Mode shape
1	68.65	73.92		7	419.50	6.12	
2	139.60	0		8	426.72	0	
3	206.86	0		9	435.16	0	
4	230.64	0		10	466.40	0	
5	269.99	8.46		11	731.31	6.72	
6	354.27	0		12	731.72	0	

In this paper, the order of the equations of motion was reduced using the first two symmetric modes (mode 1 and mode 5).

Accordingly, Eq.(34) can be written as

$$\tilde{\mathbf{K}}_e = \begin{bmatrix} 3b_{111}^1 E [q_1 q_1] + & b_{112}^1 E [q_1 q_1] + \\ 2b_{112}^1 E [q_1 q_2] + & 2b_{122}^1 E [q_1 q_2] + \\ b_{122}^1 E [q_2 q_2] & 3b_{222}^1 E [q_2 q_2] \\ 3b_{111}^2 E [q_1 q_1] + & b_{112}^2 E [q_1 q_1] + \\ 2b_{112}^2 E [q_1 q_2] + & 2b_{122}^2 E [q_1 q_2] + \\ b_{122}^2 E [q_2 q_2] & 3b_{222}^2 E [q_2 q_2] \end{bmatrix} \quad (37)$$

To ensure the symmetry of the matrix $\tilde{\mathbf{K}}_e$ and

through comparison of terms with like powers in q_j and q_k (and taking into account that q_j and q_k can be arbitrary), relationships between the nonlinear cubic coefficients are found.

$$\begin{aligned} 3b_{111}^2 &= b_{112}^1 \\ b_{112}^2 &= b_{122}^1 \\ b_{122}^2 &= 3b_{222}^1 \end{aligned} \quad (38)$$

The nonlinear stiffness coefficients are shown in Table 4, which are in good agreement with Eq.(38). The validity of the method is verified again. The modal linear stiffness, equivalent stiffness, and total equivalent stiffness matrices at 160 dB are given in Table 5.

Table 4 Modal nonlinear cubic stiffness coefficient of metal stiffened plate

Modal	q_1^3	$q_1^2 q_2$	$q_1 q_2^2$	q_2^3
1	$b_{111}^1 = 3.9595 \times 10^{12}$	$b_{112}^1 = -8.6755 \times 10^{11}$	$b_{122}^1 = 2.3572 \times 10^{13}$	$b_{222}^1 = 1.0980 \times 10^{12}$
2	$b_{111}^2 = -2.9912 \times 10^{11}$	$b_{112}^2 = 2.3600 \times 10^{13}$	$b_{122}^2 = 3.2997 \times 10^{12}$	$b_{222}^2 = 6.3349 \times 10^{13}$

Table 5 Modal linear stiffness, equivalent stiffness, and total equivalent stiffness matrices obtained for the stiffened plate at an acoustic load of 160 dB

Modal linear stiffness matrix	Equivalent stiffness matrix	Total equivalent stiffness matrix
$\begin{bmatrix} 1.8600 \times 10^5 & 0 \\ 0 & 2.8773 \times 10^6 \end{bmatrix}$	$\begin{bmatrix} 3.8921 \times 10^6 & -7.8251 \times 10^4 \\ -8.7251 \times 10^4 & 9.6467 \times 10^6 \end{bmatrix}$	$\begin{bmatrix} 4.0781 \times 10^6 & -7.8251 \times 10^4 \\ -8.7251 \times 10^4 & 1.2524 \times 10^7 \end{bmatrix}$

3.2 Result and analysis

The RMS fringe of displacement and acceleration responses obtained by linear analysis and EL analysis are shown in Table 6. The stiffened plate model in this paper has the same mass as the aluminum plate model in Ref.[18]. The part of the material where the thickness of the stiffened plate decreases relative to the aluminum plate is used as the stiffeners. Compared with the displacement response of the metal plate in Ref.[18], the linear and EL analysis results are reduced by 0.32×10^{-2} m and 0.10×10^{-3} m, respectively, since the stiffeners increase the stiffness of the structure. The center displacement is obtained by linear and EL analyses. The frequencies corresponding to the resonant peaks obtained in the EL analysis continuously shift upward with the increasing pressure loading, and the difference between the fundamental and second

mode frequencies is not constant, which is similar to the laminated plates in Ref.[18]. So, in this paper only the displacement response power spectral density (PSD) in the direction of Z of Node 165 in the center of stiffened plate is shown in Fig.3 at acoustic pressure loads of 160 dB. The acceleration response PSD in the direction of Z of the Node 165 in the center of stiffened plate under 160 dB is shown in Fig.4.

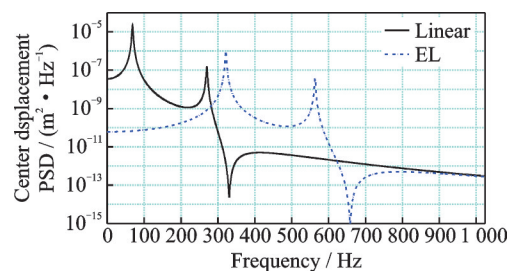
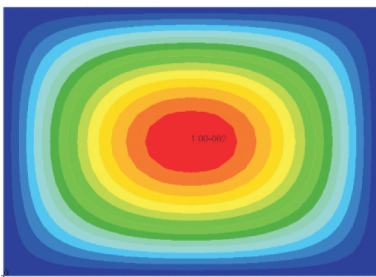
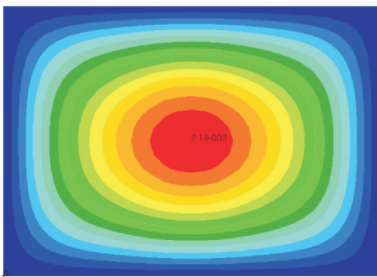
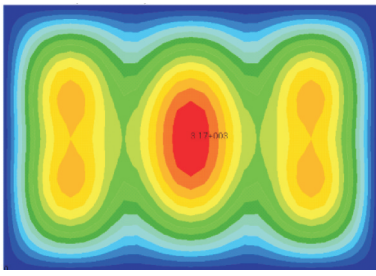
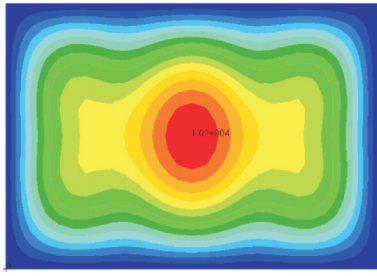


Fig.3 Comparison of displacement PSD in Z direction of Node 165 obtained by linear and EL analyses of stiffened plate at 160 dB

Table 6 Displacement and acceleration response RMS of metal stiffened plates by linear and EL analyses at 160 dB acoustic load

Fringe	Linear analysis	EL analysis
Displacement response RMS	 <p>Max: 1.00×10^{-2} m</p>	 <p>Max: 2.18×10^{-3} m</p>
Acceleration response RMS	 <p>Max: 3.17×10^3 m/s²</p>	 <p>Max: 1.02×10^4 m/s²</p>

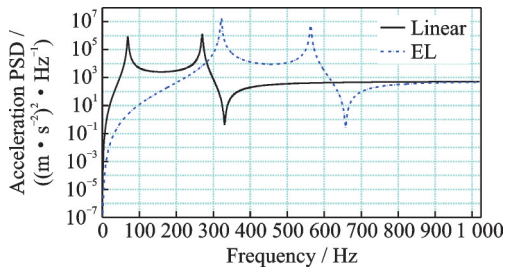
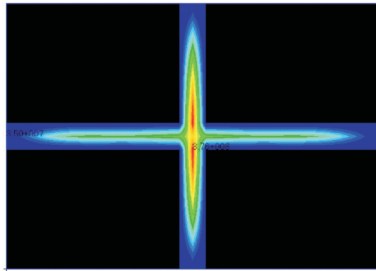
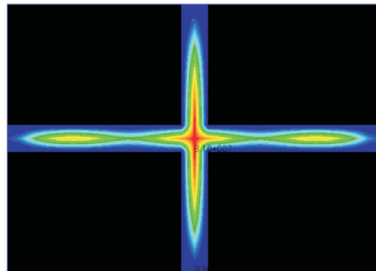
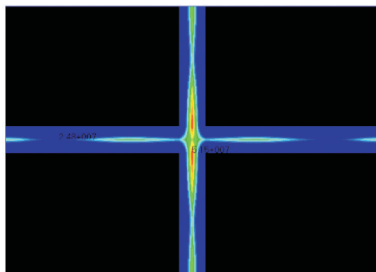
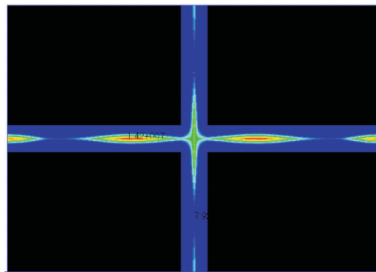


Fig.4 Comparison of acceleration PSD in Z direction of Node 165 obtained by linear and EL analyses of stiffened plate at 160 dB

It is found from Table 7 that the stress response of the beam element predicted by the linear analysis is larger than that by the EL analysis, that is, the linear analysis overestimates the response value. The finite element model for beam and plate assembly established in this paper can analyze the stress response at different locations of cross section of the beam element. As shown in Fig.1(b), the re-

sponse results of point C and point D on the cross section of beam element are significantly different from the middle surface. The stress response RMS value of point C, which is far from the middle surface of the plate, is greater than that of point D, which is near the middle surface of the plate. The PSD distribution of stress response at point C and point D in the cross-section of beam element 608 (along the direction of the short side) obtained from linear and EL analyses are shown in Figs.5, 6. The PSD distribution of stress response at point C and point D in the cross-section of beam element 575 (along the long side direction) obtained by linear and EL analyses are shown in Figs.7, 8. By contrastive analysis from Figs.5—8, it is found that the stress response value of beam element 608, which is in short-side direction, is larger than that of beam element 575, which is in long-side direction.

Table 7 Beam stress responses RMS fringe by linear and EL analysis at 160 dB acoustic load

Fringe	Linear analysis	EL analysis
Stress response RMS at point C	 <p>Max: 3.76×10^8 Pa, Min: 3.50×10^7 Pa</p>	 <p>Max: 8.10×10^7 Pa, Min: 9.80×10^6 Pa</p>
Stress response RMS at point D	 <p>Max: 5.15×10^7 Pa, Min: 2.48×10^7 Pa</p>	 <p>Max: 1.42×10^7 Pa, Min: 7.92×10^6 Pa</p>

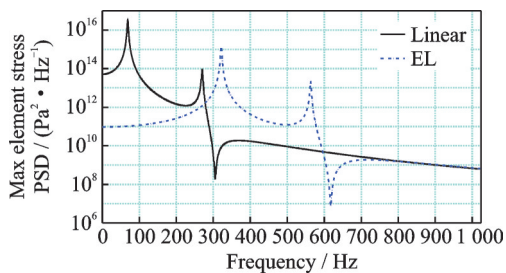


Fig.5 PSD distribution of stress response at point C in cross-section of beam element 608 obtained from linear and EL analyses at 160 dB acoustic load

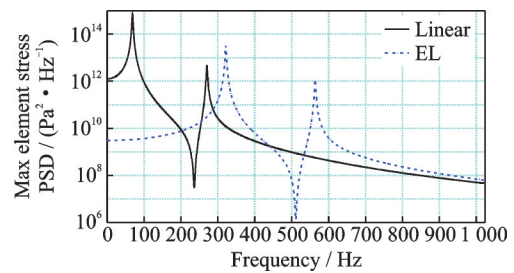


Fig.6 PSD distribution of stress response at point D in cross-section of beam element 608 obtained from linear and EL analyses at 160 dB acoustic load

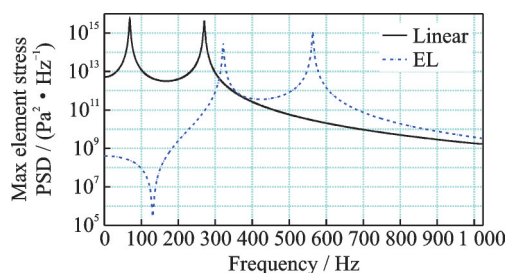


Fig.7 PSD distribution of stress response at point *C* in cross-section of beam element 575 obtained from linear and EL analyses at 160 dB acoustic load

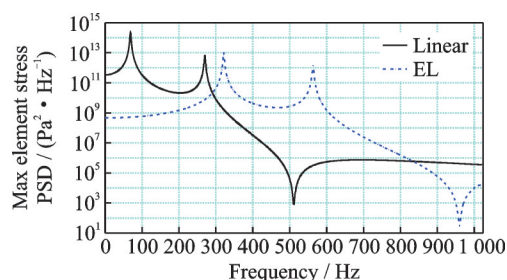
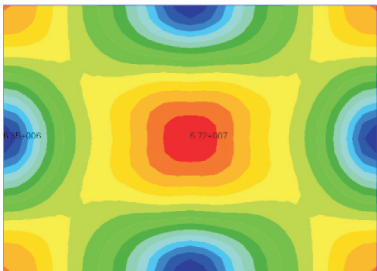
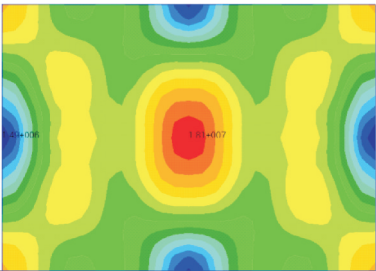
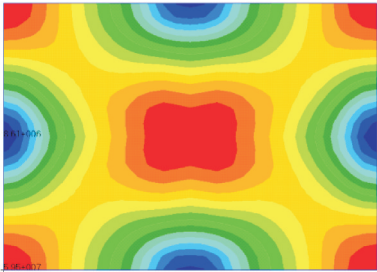
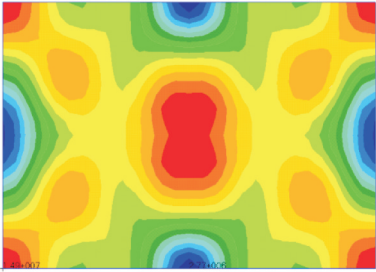


Fig.8 PSD distribution of stress response at point *D* in cross-section of beam element 575 obtained from linear and EL analyses at 160 dB acoustic load

The stress response RMS of shell elements with/without stiffeners, obtained by linear analysis and EL analysis at 160 dB acoustic pressure are listed in Table 8. The Von-Mises stress responses of the shell elements with/without stiffeners are significantly different. Because of the beam element bear-

ing part of the stress, the maximum stress of the shell elements with stiffeners is not in the middle. The stress response PSD distribution results of shell element 140 obtained by linear and EL analyses are shown in Fig.9, where $-Z$ is the unstiffened surface and $+Z$ is the stiffened surface.

Table 8 Stress responses RMS fringe on surface with/without stiffeners of metal stiffened plates by linear and EL analyses at 160 dB acoustic load

Fringe	Linear analysis	EL analysis
Von-Mises stress RMS of surface shell without stiffeners	 <p>Max: 6.72×10^7 Pa, Min: 6.35×10^6 Pa</p>	 <p>Max: 1.81×10^7 Pa, Min: 1.49×10^6 Pa</p>
Von-Mises stress RMS of surface shell with stiffeners	 <p>Max: 5.95×10^7 Pa, Min: 8.61×10^6 Pa</p>	 <p>Max: 1.49×10^7 Pa, Min: 2.77×10^6 Pa</p>

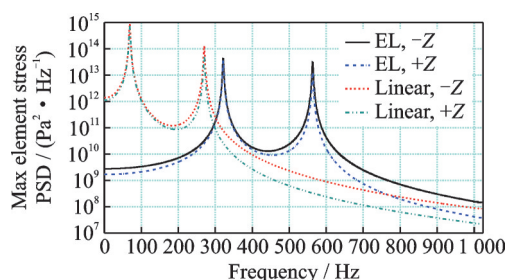


Fig.9 Von-Mises stress responses PSD of shell element 140 by linear and EL analyses at 160 dB acoustic load

4 Conclusions

The present study proposed an improved ROM-EL-FEM method to predict the geometrically nonlinear random response of simply-supported rectangular stiffened plates. The conclusions can be drawn as follows.

(1) The statistical dynamic response of shell elements and beam elements in the stiffened plates

can be obtained, respectively. The stiffeners have significant influence on vibration modes of thin plate. There are obvious differences between the stress response of the shell element at the stiffened surface and unstiffened surface. Because the stiffeners enhance the stiffness of the structure, the displacement response of the stiffened plates is reduced compared with that of the unstiffened plates of the same mass in Ref.[18].

(2) Because the stiffened plate present in this paper belongs to weak stiffened plate, its nonlinear characteristic is similar to that of thin plate. Nonlinearity in the vibration response of the stiffened plates is due to transverse deflection and in-plane stretching, which increases the stiffness of the structure, and consequently diminishes the displacement response. So, the frequencies corresponding to the resonant peaks obtained by EL analysis are higher than those obtained by linear analysis. The linear analysis do not account for this effect, which results in the prediction of exaggerated displacement responses under high acoustic pressure loading, leading to excessively conservative designs.

(3) The geometric nonlinearity plays an important role in the random vibration response of stiffened plates, particularly at high acoustic pressure loading. For the prediction of nonlinear random vibration response of stiffened plates, the basic model data have been given in this paper, which can contribute to analysis of the geometrically nonlinear random response for similar structures.

References

- [1] NEMETH M P. A treatise on equivalent-plate stiffnesses for stiffened laminated-composite plates and plate-like lattices: 216882 NASA TP[R]. Hanover, MD, USA:Langley Research Center, 2011.
- [2] MA N, WANG R, LI P. Nonlinear dynamic response of a stiffened plate with four edges clamped under primary resonance excitation[J]. *Nonlinear Dynamics*, 2012, 70(1): 627-648.
- [3] CHEN Z, WANG R, CHEN L, et al. Strongly nonlinear free vibration of four edges simply supported stiffened plates with geometric imperfections[J]. *Journal of Mechanical Science and Technology*, 2016, 30(8): 3469-3476.
- [4] CHO D S, KIM B H, KIM J, et al. Forced vibration analysis of arbitrarily constrained rectangular plates and stiffened panels using the assumed mode method[J]. *Thin-Walled Structures*, 2015, 90: 182-190.
- [5] SHEIKH A H, MUKHOPADHYAY M. Geometric nonlinear analysis of stiffened plates by the spline finite strip method[J]. *Computers & Structures*, 2000, 76(6): 765-785.
- [6] SHEIKH A H, MUKHOPADHYAY M. Linear and nonlinear transient vibration analysis of stiffened plate structures[J]. *Finite Elements in Analysis and Design*, 2002, 38(6): 477-502.
- [7] MITRA A, SAHOO P, SAHA K. Nonlinear vibration analysis of simply supported stiffened plate by a variational method[J]. *Mechanics of Advanced Materials and Structures*, 2013(20): 373-396.
- [8] QING G, QIU J, LIU Y. Free vibration analysis of stiffened laminated plates[J]. *International Journal of Solids and Structures*, 2006, 43(6): 1357-1371.
- [9] LI Y, MULANI S B, FEI Q, et al. Vibro-acoustic analysis under stationary and non-stationary random excitations with KLE/FEM/BEM[J]. *Aerospace Science and Technology*, 2017, 66: 203-215.
- [10] DOGAN V. Nonlinear vibration of FGM plates under random excitation[J]. *Composite Structures*, 2013, 95: 366-374.
- [11] ROBINSON J H, CHIANG C K, RIZZI S A. Nonlinear random response prediction using MSC / NASTRAN: NASA Technical Memorandum 109029[R]. [S. l.]: NASA Langley Research Center, 1993.
- [12] RIZZI S A, PRZEKOP A. The effect of basis selection on static and random acoustic response prediction using a nonlinear modal simulation: NASA/TP-2005-213943 [R]. [S. l.]: NASA Langley Research Center, 2005.
- [13] PRZEKOP A, GUO X, RIZZI S A. Alternative modal basis selection procedures for reduced-order nonlinear random response simulation[J]. *Journal of Sound and Vibration*, 2012, 331(17): 4005-4024.
- [14] KIM K, RADU A G, WANG X Q, et al. Nonlinear reduced order modeling of isotropic and functionally graded plates[J]. *International Journal of Non-linear Mechanics*, 2013, 49: 100-110.
- [15] MIGNOLET M P, PRZEKOP A, RIZZI S A, et al. A review of indirect/non-intrusive reduced order modeling of nonlinear geometric structures[J]. *Journal of Sound and Vibration*, 2013, 332(10): 2437-2460.
- [16] PARANDVAR H, FARID M. Nonlinear reduced order modeling of functionally graded plates subjected to random load in thermal environment[J]. *Composite Structures*, 2015, 126: 174-183.

- [17] PRZEKOP A, RIZZI S A. Dynamic snap-through of thin-walled structures by a reduced-order method[J]. AIAA Journal, 2007, 45(10): 2510-2519.
- [18] YANG S, YANG Q. Geometrically nonlinear random vibration responses of laminated plates subjected to acoustic excitation[J]. AIAA Journal, 2018, 56(7): 2827-2839.
- [19] RIZZI S A, MURAVYOV A A. Equivalent linearization analysis of geometrically nonlinear random vibrations using commercial finite element codes: NASA/TP-2002-211761 [R]. [S. l.]: NASA Langley Research Center, 2002.
- [20] RIZZI S A, MURAVYOV A A. Improved equivalent linearization implementations using nonlinear stiffness evaluation: NASA/TM-2001-210838 [R]. [S. l.]: NASA Langley Research Center, 2001.
- [21] WIJCKER J J. Spacecraft structures[M]. Berlin Heidelberg: Springer-Verlag, 2008.
- [22] HOLLKAMP J J, GORDON R W, SPOTTSWOOD S M. Nonlinear modal models for sonic fatigue response prediction: A comparison of methods[J]. Journal of Sound and Vibration, 2005, 284(3/4/5): 1145-1163.
- [23] MURAVYOV A A, RIZZI S A. Determination of nonlinear stiffness with application to random vibration of geometrically nonlinear structures[J]. Computers & Structures, 2003, 81(15): 1513-1523.
- [24] MSC Software Corporation. MD/MSC Nastran 2010 quick reference guide[M]. Santa Ana: MSC Software Corporation, 2010.

Acknowledgements This work was supported by the Na-

tional Natural Science Foundations of China (Nos.11872079, 11572109), the Science and Technology Project of Hebei Education Department (No. QN2019135), Advanced Talents Incubation Program of the Hebei University (No. 521000981285).

Authors Dr. YANG Shaochong received the Ph.D. degree in mechanics from Beijing University of Technology, Beijing, China, in 2018. He is currently a lecturer of College of Civil Engineering and Architecture, Hebei University. His current research interests include structural dynamics, computational mechanics.

Prof. YANG Qingsheng received the Ph.D. degree in mechanics from Dalian University of Technology, China, in 1992. He is currently a full professor of Department of Engineering Mechanics, Beijing University of Technology. His current research interests include mechanical properties of novel materials and structures, macro-and micro-mechanics of composites, multi-scale computational mechanics method and application, multi-filed coupling performance of intelligent and biological materials.

Author contributions Dr. YANG Shaochong designed the study, built the models and wrote the manuscript. Mr. LI Youchen contributed to data collect and analysis. Prof. YANG Qingsheng guided the writing of the article, and revised the manuscript. Prof. WANG Jianmin contributed to the discussion and background of the study. All authors commented on the manuscript draft and approved the submission.

Competing interests The authors declare no competing interests.

(Production Editor: SUN Jing)

噪声作用下加筋板的几何非线性随机响应

杨少冲¹, 李有晨¹, 杨庆生², 王建民³

(1. 河北大学建筑工程学院, 保定 071002, 中国; 2. 北京工业大学工程力学系, 北京 100124, 中国;
3. 北京强度环境研究所可靠性与环境工程技术重点实验室, 北京 100076, 中国)

摘要:提出了一种降阶模型、等效线性化和有限元相结合的方法,对噪声荷载作用下加筋板的几何非线性随机振动进行分析。基于大挠度有限元公式,得到加筋板的非线性运动方程。为了减少计算量,建立了结构的降阶模型,然后通过DMAP语言编程将等效线性化技术集成到NASTRAN有限元软件中。针对加筋板建立了梁-板组合的有限元模型,梁单元与壳单元共用节点,并确定梁的偏置和截面属性。本方法可以分别获得梁、板单元的应力响应均方根值,并可得到加筋板有/无加筋面各自的应力分布。最后对比分析了分别由线性和等效线性化方法得出的统计动态响应结果。结果表明,该方法可用于分析加筋板的几何非线性随机响应。几何非线性因素在加筋板随机振动响应预测中起着重要的作用,尤其是在强噪声载荷下。

关键词:加筋板; 噪声载荷; 几何非线性; 随机振动; 等效线性化